Chronic oral administration of P. gingivalis induces microglial activation and degeneration of dopaminergic neurons possibly through increase in gut permeability and peripheral IL-17A in LRRK2 R1441G mice

Yu-kun Feng
Sun Yat-Sen University
Yan-Wen Peng
Sun Yat-Sen University
Qiong-Li Wu
Sun Yat-Sen University
Feng-Yin Liang
Sun Yat-Sen University
Hua-Jing You
Sun Yat-Sen University
Yi-Wei Feng
Sun Yat-Sen University
Ge Li
Guangdong Pharmaceutical University
Xue-jiao Li
Guangdong Pharmaceutical University
Shu-Hua Liu
Sun Yat-Sen University
Yong-Chao Li
Guangdong Pharmaceutical University
Yu Zhang
Guangdong Pharmaceutical University
Zhong Pei (peizhong@mail.sysu.edu.cn)
Sun Yat-Sen University

Research

Keywords: chronic periodontitis, Parkinson's disease, dopaminergic neurons, R144G LRRK2, IL-17-IL-17RA axis

Posted Date: June 15th, 2020

DOI: https://doi.org/10.21203/rs.3.rs-34883/v1

Version of Record: A version of this preprint was published on November 19th, 2020. See the published version at https://doi.org/10.1186/s12974-020-02027-5.

Abstract

Background

The R1441G mutation in the leucine-rich repeat kinase 2 (LRRK2) gene results in late-onset Parkinson's disease (PD). Peripheral inflammation and gut microbiota are closely associated with the pathogenesis of PD. Chronic periodontitis is a common type of peripheral inflammation, which is associated with PD. *Porphyromonas gingivalis* (Pg), the most common bacterium causing chronic periodontitis, can cause alteration of gut microbiota. It is not known whether Pg-induced dysbiosis plays a role in the pathophysiology of PD.

Methods

In this study, live Pg were orally administrated to animals, three times a week for one month. Pg-derived lipopolysaccharide (LPS) was used to stimulate peripheral blood mononuclear cells in vitro. The effects of oral Pg administration on the gut and brain were evaluated through behaviors, morphology, and cytokine expression.

Results

Dopaminergic neurons in the substantia nigra were reduced and activated microglial cells were increased in R1441G mice given oral Pg. In addition, an increase in mRNA expression of tumor necrosis factor (TNF-α) and interleukin-1 β (IL-1β) as well as protein level of α-synuclein together with a decrease in zonula occludens-1 (Zo-1) were detected in the colon in Pg-treated R1441G mice. Furthermore, serum interleukin-17A (IL-17A) and brain IL-17 receptor A (IL-17RA) were increased in Pg-treated R1441G mice.

Conclusions

These findings suggest that LRRK2 causes gut leakage and further mediates peripheral IL-17A response in Pg-treated animals. We, thus, put forward the hypothesis that IL-17A in the serum may result in activation of the IL-17A-IL-17RA axis that aggravates dysfunction of dopaminergic neurons and provokes microglial activation in LRRK2 R1441G mice.

Background

Parkinson's disease (PD) is the second most common neurodegenerative disease that results in a progressive movement disorder characterized by slowness, rigidity, gait difficulty, and rest tremors [1]. Degeneration of dopaminergic neurons in the substantia nigra pars compacta (SNpc) is one of the pathological hallmarks of PD [2–3]. Although the exact cause of PD remains poorly understood, it is

generally believed that complex interactions between genetic and environmental factors contribute its development.

Leucine-rich repeat kinase 2 (LRRK2) mutants are the most common genetic factors in the pathogenesis of PD [4]. Substantial evidence suggests that mutant LRRK2 strongly activates brain immune cells, which in turn mediate neurodegeneration through neuroinflammation [5–6]. Interestingly, LRRK2 has been also linked to several systemic inflammatory diseases, such as inflammatory bowel disease and leprosy [7–8]. Activation of LRRK2, however, has been reported to induce opposite effects in the brain and the periphery. For example, activation of LRRK2 protects against infection in the gut, but causes neurodegeneration in the brain [9–10].

Recently, chronic systemic inflammatory diseases have been linked to the risk of developing PD. Periodontal disease is a common chronic inflammatory disease and is associated with PD [11–13]. Interestingly, *Porphyromonas gingivalis* (Pg), the major periodontal pathogen, induces dysbiosis of gut microbiota [14–15].

The relationship between intestinal function disorder and PD has attracted much attention [16–17]. Until now, the link between the two diseases was based only on motor disturbances caused by PD, which could lead to progression of periodontal disease [12–13]. However, whether periodontal disease can have an influence on initiation and progression of PD through the intestinal pathway and the underlying mechanism remain unclear.

Recent studies suggest that peripheral lymphocytes may play a central role in the pathophysiology of PD [18]. For example, interleukin-17A (IL-17A) level was significantly increased in the serum of patients with PD [19–21]. Furthermore, IL-17A could induce human induced pluripotent stem cell-derived midbrain neuronal cell death, possibly through IL-17 receptor A (IL-17RA) [19–20]. IL-17A is mainly driven by Th17 lymphocytes. Interestingly, Th17 cells have been linked to several immune-related diseases, including periodontal disease [22–23]. Th17 cells are also essential for normal defense against gut pathogens [24].

Therefore, we hypothesized that oral Pg might induce peripheral inflammatory responses leading to degeneration of dopaminergic neurons through the gut in LRRK2 R1441G mice.

Materials And Methods

Animals

All animal procedures were performed according to the Guide for the Care and Use of Laboratory Animals of Sun Yat-sen University (Guangzhou, China). All animals were housed in a specific pathogen-free facility with a 12:12 h light/dark cycle, *ad libitum* food and water. In this study, 3- to 4-month-old FVB/NJ, and FVB/N-Tg (LRRK2*R1441G)135Cjli/J mice were purchased from Jackson Laboratory (Bar Harbor, ME, USA) and crossed in the Guangdong Laboratory Animals Monitoring Institute (Guangzhou, China). At one month, all littermates were genotyped. Genotyping was done by polymerase chain reaction (PCR) of

tail DNA using a protocol from Jackson Laboratory. A total of 40 mice were used in this study and assigned to four groups: FVB/N + carboxymethyl cellulose (F + C), FVB/N + Pg (F + Pg), R1441G + C, and R1441G + Pg.

Pg cultures and administration

Pg was cultured in broth (Brian Heart Infusion, L-cysteine hydrochloride monohydrate, yeast extract, and chloroproto-ferriheme, Sigma-Aldrich, St. Louis, Missouri, USA). After that, Pg was placed in an anaerobic container for 48 h at 37°C. A total of 10^9 colony-forming units of live Pg was suspended in 0.1 ml phosphate-buffered saline (PBS) with 2% carboxymethyl cellulose (CMC) (Sigma-Aldrich), and given to each mouse by gavage three times a week for about a month, as described previously [14-15]. The control group was administered 0.1 ml PBS with 2% CMC without Pg. After administration, all mice were allowed to eat and drink ad libitum.

Behavioral tests

Rotarod test

Animals were placed on an accelerating rotarod (Xin Ruan, Shanghai, China) with an accelerated speed of 4–40 rpm for 5 min, and the latency to fall was recorded each time. Animals were tested three times a day for three consecutive days, allowing for two days of training and acclimatization. A resting time of at least 30 min was given between trials. The results are presented as the average of the three times.

Open field

Animals were placed in the chamber (45 × 45 × 45 cm) with a video camera (Xin Ruan, Shanghai, China). Every mouse was carefully placed in the center of the chamber and allowed to freely explore the chamber. Animals were tested for two consecutive days, allowing for one day of training and acclimatization. The movement of mice was filmed and analyzed automatically for 10 min.

Immunofluorescence

Brain tissue and colon were removed, fixed, and dehydrated to further process for immunofluorescence. After blocking for 1 h at room temperature, brain sections were incubated with primary antibodies overnight at 4°C. The primary antibodies used in this study were tyrosine hydroxylase (TH) (MAB318, Millipore, Bedford, MA, USA), allograft inflammatory factor 1 (Iba1) IgG (019-19741, Wako, Japan), cleaved active caspase-3 (9661, Cell Signaling Technology, Danvers, MA, USA), LRRK2 (MJFF2 [c41-2]) (ab133474, Abcam, Cambridge, UK), MAP2 IgG (ab32454, Abcam), Iba1 IgG (MA5-27726, Thermo Fisher Scientific, Waltham, MA, USA) and IL-17RA IgG (ab180904, Abcam). Subsequently, the sections were incubated with Alexa 488 or 555-conjugated secondary antibodies (4408, 4413, Cell Signaling Technology) for another 1 h at room temperature. Finally, sections were viewed under a Nikon microscope (Japan). The numbers and density of target cells were measured using ImageJ v1.51 software.

Western blot

The brain was cut into sections in the mold. The colon and the SN tissue were homogenized in radioimmunoprecipitation assay buffer (Thermo Scientific) with phenylmethanesulfonyl fluoride (1:100) and phosphatase inhibitors (Roche, Basel, Switzerland) in an ultrasonic disintegrator. Homogenates were incubated on ice for 30 min and centrifuged at 12,000 rpm for 25 min at 4°C. The protein concentration was determined using the Pierce BCA Protein Assay Kit (Thermo Scientific). Equal quantities of proteins were separated by sodium dodecyl sulfate polyacrylamide gel electrophoresis and transferred to polyvinylidene fluoride membranes. The membranes were blocked with 5% non-fat dry milk or bovine serum albumin for 1 h at room temperature and incubated with primary antibody overnight at 4°C. The primary antibodies used were LRRK2 (MJFF2 [c41-2]) IgG (ab133474, Abcam), phospho-LRRK2 ^{S935} IgG (ab133450, Abcam), MAP2 IgG (ab32454, Abcam), cleaved active caspase-3 IgG (BF0711, Affinity, China), and IL-17RA IgG (ab180904, Abcam). α-tubulin was used as a loading control. After incubating with anti-rabbit or anti-mouse secondary antibodies (7074, 7076, Cell Signaling Technology) for 1 h, the bands were visualized using the electrochemiluminescence detection reagents (Millipore) on an Amersham Imager 600 (Amersham Biosciences, USA). The relative density of protein was analyzed by ImageJ v1.51 software.

Peripheral blood mononuclear cell(PBMC) cultures and stimulation

Spleens were mechanically disrupted and filtered through a 40 μm cell-strainer (Falcon, BD Biosciences, Durham, NC, USA) and isolated by Ficoll-Hypaque (Tianjin HaoYang Biological Manufacture Co, Ltd, Tianjin, China) density gradient centrifugation to procure PBMCs, according to the manufacturer's instructions. The cells (2×10^6/ml) were suspended in complete roswell park memorial institute 1640 medium and stimulated for 24 and 48 h with or without Pg-LPS (1 μg/ml, 2 μg/ml, 4 μg/ml, 8 μg/ml; SMB00610, Sigma-Aldrich) in the presence of anti-CD3 mAb and anti-CD28 mAb (553057, 553294, BD Biosciences) in round-bottomed 96-well plates, (200 μl/well) at 37°C and 5% CO_2.

Enzyme-linked immunosorbent assay (ELISA)

The levels of IL-17A in serum from Pg-treatment mice and supernatant from Pg-LPS-stimulated PBMCs were measured with an ELISA kit (88-7371, BioLegend, CA, USA). ELISA assays were performed according to the manufacturer's instructions. Data were collected by an ELISA reader under a wavelength of 450 nm. The results are shown as the mean readings from triplicate wells.

Quantitative real-time polymerase chain reaction (RT-qPCR)

Total RNA from large intestines was extracted using TRI Reagent (Invitrogen, Carlsbad, CA, USA) and was quantified using a NanoDrop 2000 (Thermo Fisher Scientific). cDNA was synthesized with Novoscript® Plus All-in-one-1st Strand cDNA Synthesis SuperMix (Novoprotein, Shanghai, China), according to the manufacturer's instructions. This cDNA was subsequently used for RT-qPCR analysis using specific validated primers (Takara, Japan) and SYBR qPCR Supermix Plus (Novoprotein) in eight straight tubes in

the StepOnePlus instrument (Thermo Fisher Scientific). StepOnePlus™ software (Thermo Fisher Scientific) was used to analyze the standards and carry out the quantification. Glyceraldehyde-3-phosphate dehydrogenase (GAPDH) mRNA was used as the normalizing gene. The mRNA levels for each gene were expressed as $2^{-\Delta\Delta Ct}$, denoting fold-change. Primer sequences were: GAPDH (forward) 5¢-TCAATGAAGGGGTCGTTGAT-3¢, (reverse) 5¢-CGTCCCGTAGACAAAATGGT-3¢; interleukin-1β (IL-1β) (forward) 5¢-TGCCACCTTTTGACAGTGATG-3¢, (reverse) 5¢-ATACTGCCTGCCTGAAGCTC-3¢. tumor necrosis factor α (TNF-α) (forward) 5¢-GACGTGGAACTGGCAGAAGAG-3¢, (reverse) 5¢-TTGGTGGTTTGTGAGTGTGAG-3¢; and zonula occludens-1 (Zo-1) (forward) 5¢-AGCGAATGTCTAAACCTGGG-3¢, (reverse) 5¢- TCCAACTTGAGCATACACAGG-3¢.

Statistical analysis

Data were analyzed with one-way ANOVA with Tukey's multiple comparisons test using GraphPad Prism 6.0 software. The results are expressed as the mean ± SEM. Statistical significance was set at $P < 0.05$.

Results

1. Oral Pg induced dopaminergic neuronal degeneration in the SNpc of mutant LRRK2 mice

To examine whether oral Pg can induce dopaminergic neuronal degeneration, Pg was administrated orally to FVBN mice and LRRK2 R1441G transgenic mice for a month. Immunofluorescence TH staining was used to examine loss of SNpc dopaminergic cells. We found that there was a significant loss of TH + neurons in the SNpc in R1441G mice, but not in FVBN mice (Fig. 1a). Confocal immunofluorescence imaging revealed active caspase-3 in the cytoplasm and cell nucleus of TH + SNpc dopaminergic neurons of LRRK2 R1441G mice, but not FVBN mice (Fig. 1b). Immunoblot further confirmed that protein level of cleaved active caspase-3 was greatly increased in the SN of LRRK2 R1441G mice after Pg treatment compared to FVBN mice (Fig. 1c). In addition, LRRK2 R1441G mice exhibited a significant reduction in the immunofluorescence intensity of SNpc MAP2 + dendrite (Fig. 1d), which was accompanied by the reduction in MAP2 + protein level (Fig. 1e). In contrast, the immunofluorescence intensity of SNpc MAP2 + dendrite was not significantly altered in FVBN + Pg. To further determine whether inflammation-induced neuronal loss is mutation specific, Pg was administered to mice overexpressing human wild-type LRRK2 (WT-OX). We found that there were no significant differences in TH + number and expression levels of MAP2 + protein between Pg-treated WT-OX and WT-OX mice (Supplementary Figs. 1a, b), thereby suggesting that oral Pg-induced neurodegeneration was mutant LRRK2-dependent. Meanwhile, there were no significant differences in the rotarod and open field tests among these groups (Supplementary Fig. 1c).

2. Oral Pg increased microglial activation in the SNpc of mutant LRRK2 mice

Over-activation of microglia has been linked to neurodegeneration in PD [25–26]. In the present study, there was a significant increase in the number of activated Iba1-positive microglia in the SNpc in R1441G

mice compared to FVBN and WT-OX mice, one month following treatment with oral Pg (Fig. 2a, Supplementary Fig. 2a).

3. Oral Pg increased LRRK2 activation in the SN of R1441G mice

Mutant LRRK2 has been implicated in neuronal cell death and microglial inflammatory response of SNpc [5, 10]. In this study, both LRRK2 and LRRK2^{p935} were significantly increased in the SN of Pg-treated R1441G mice compared to Pg-treated FVBN mice (Fig. 3a, b). Although LRRK2 protein expression was also increased in the SN of Pg-treated WT-OX mice, LRRK2^{p935} was not altered in WT-OX after Pg treatment (Supplementary Fig. 2c). Double immunofluorescence staining using anti-LRKK2, anti-TH, and anti-Iba1 was performed to visualize the co-localization of LRRK2 in SNpc dopaminergic neurons and microglia. Consistent with western blots, the immunosignal of LRRK2 was evident in Pg-treated R1441G mice. In addition, LRRK2 was partially co-localized with TH + neurons and Iba1 + microglia (Figs. 3c, d).

4. Mutant LRRK2 exacerbated Pg-induced peripheral IL-17A secretion and IL-17RA upregulation

IL-17A has been linked to the activation of LRRK2 [27]. We first examined the serum levels of IL-17A in animals receiving either CMC or Pg. There was no significant difference in IL-17A between FVBN and R1441G mice following CMC treatment (Fig. 4a). However, serum IL-17A was significantly increased in R1441G mice compared to FVBN mice following oral administration of Pg (Fig. 4a). Consistently, IL-17A was significantly increased in the supernatant of PBMCs from R1441G mice stimulated by Pg-derived LPS compared with FVBN mice (Fig. 4b). However, IL-17A protein level remained unchanged in the SN (Supplementary Fig. 2d). Instead, IL-17RA protein level was elevated in the SN of R1441G mice with Pg compared with FVBN mice (Fig. 4c). In addition, IL-17RA was co-localized with TH in the SN of R1441G mice with Pg (Fig. 4d)

5. Pg-treatment increased the accumulation of α-synuclein in neurons of the colon and induced activation of LRRK2

Emerging evidence suggests that α-synuclein accumulates in neurons of the gut prior to the brain in PD [17, 28]. Although histological analysis revealed normal morphology of the colon and small intestine in all groups (Supplementary Fig. 3a), we found that the α-synuclein in the myenteric plexus of the colon was higher in Pg-treated R1441G mice than in control mice (Fig. 5a). There was no detectable α-synuclein in the brain and small intestine (data not shown). Furthermore, immunoblot analysis demonstrated a significant increase in LRRK2 and LRRK2^{935} protein levels in the colon of Pg-treated R1441G mice compared to each of the other three groups of mice. Besides, oral administration of Pg led to a significant increase in mRNA expression of TNF-a, IL-1β, and Zo-1 in the colon of R1441G mice, but not FVBN mice.

Discussion

LRRK2 is highly expressed in immune cells and mutation of LRRK2 has been linked to both intestinal inflammatory disease and PD [5, 29–30]. In this study, we investigated the contribution of oral Pg to the

pathogenesis of mutant LRRK2-PD in LRRK2 (R1441G) mice. Although oral Pg induced a mild inflammatory response in the intestine, it caused a significant loss of dopaminergic neurons and profound microglial activation in the SNpc. In addition, oral Pg resulted in an IL-17A immune response in the periphery and upregulation of IL-17RA protein level of dopaminergic neurons, thereby suggesting that the interaction between IL-17A with IL-17RA may be responsible for neurodegeneration and neuroinflammation in LRRK2-associated PD. Furthermore, these oral Pg-mediated harmful effects are accompanied by an increase in $LRRK2^{935}$ expression, which suggests a critical role of LRRK2 kinase in Pg-induced neuropathogenesis in LRRK2-associated PD.

Systemic inflammation has been shown to induce dopaminergic neuronal death through activation of LRRK2 [6]. We consistently found that dopaminergic degeneration was evident in R1441G animals following Pg administration. This event is mediated by aberrant LRRK2 kinase, as evidenced by an increase in $LRRK2^{935}$ expression in both the brain and colon. Interestingly, Pg-induced expression of $LRRK2^{935}$ led to profound activation of microglia, whereas the gut morphology remained intact in R1441G mice. Thus, it is intriguing how oral Pg induces neuroinflammation in the brain. In PD, α-synuclein is considered to play a pivotal role in brain-gut-microbiota axis interactions [28, 31]. Gut inflammation induces expression of α-synuclein and the latter travels along with the vague nerve to initiate the process of α-synuclein misfolding in the brain, which leads to neuroinflammation [32]. Previously, LRRK2 activity has been shown to enhance expression of α-synuclein [33–34]. Pg-mediated LRRK2 activation consistently induced expression of α-synuclein in the colon of R1441G mice. However, α-synuclein levels in the brain were not significantly different between FVBN and R1441G mice, thereby suggesting that α-synuclein may not be responsible for activation of microglia. This is in contrast to a recent observation that injection of α-synuclein fibrils in the gut mediates the spread of pathologic α-synuclein in the brain via the vagus nerve [35]. Use of different animal models may explain the discrepancy between our study and the previous study. Indeed, α-synuclein fibrils can effectively seed the formation of Lewy body-like inclusions due to their high aggregation propensity. Alternatively, gut-mediated systemic inflammation may induce brain inflammation via circulating cytokines [32, 36]. In the periphery, it has been reported that activation of LRRK2 in monocytes and macrophages modulates proinflammatory responses, such as IL-1β and TNF-a, which in turn lead to loss of the epithelial barrier function [5, 9, 37–38]. We consistently found that oral Pg induced LRRK2 activation and reduced epithelial barrier protein Zo-1. Consequently, loss of Zo-1 may evoke the release of Pg-derived LPS into the blood stream. Elevated IL-17A level has been reported in the serum from patients with PD [19–20]. Emerging evidence indicates that IL-17A can induce neuroinflammation in animal models and PD patients [39–42]. IL-17A level was consistently increased in the serum of R1441G mice with oral Pg, as well as Pg-derived LPS-stimulated PBMC from R1441G mice. Peripheral IL-17A has been reported to disrupt and cross the blood-brain-barrier [42]. However, neither IL-17A nor Th17 cells could be detected in the brain. Thus, peripheral IL-17A may be responsible for neurodegeneration. IL-17RA is required for the biological activity of IL-17A [43]. In our study, we found that IL-17RA was increased in the dopaminergic neurons of the SN. Several studies have shown that IL-17 could trigger neuronal death through IL-17RA [19]. Thus, it is likely that serum IL-17A may mediate neuronal death through interaction with IL-17RA in

Pg-induced R1441G mice. Interestingly, IL-17A has been reported to mediate dopaminergic neurons degeneration via IL-17RA in microglia in a previous study [41]. However, we did not detect any expression of IL-17RA in microglia, although reactive microglia were evident in Pg-induced R1441G mice. The differing results may be due to the use of different models in the experiments.

Microglia in a state of heightened reactivity have a vital role in PD [44]. Evidence suggests that mutant LRRK2 may enhance microglial process outgrowth and inflammatory response leading to chronic damage of dopaminergic neurons [45–46]. Our study consistently showed a significant increase in Iba1 number in R1441G LRRK2 mice. Besides, our study showed LRRK2 co-localization in microglia and neurons. We, therefore, put forward the hypothesis that activation of the IL-17A-IL-17RA axis aggravates dysfunction of dopaminergic neurons and induces microglial activation in R1441G LRRK2 animals.

Conclusions

Our results indicate that activation of LRRK2 may have an important role in gut barrier leakage and IL-17A production, and subsequently trigger neuronal death through the IL-17A-IL-17RA axis. In conclusion, our results elucidate the role of the brain-gut axis in the pathophysiology of Parkinson's disease.

Abbreviations

LRRK2
Leucine rich repeat kinase 2;
Pg
Porphyromonas gingivalis;
LPS
Lipopolysaccharide;
IBA-1
Allograft inflammatory factor 1;
IL-17A
Interleukin-17A;
IL-1β
Interleukin-1β;
Zo-1
Zonula occludens-1;
PD
Parkinson's disease;
SNpc
Substantia Nigra pars compacta;
TH
Tyrosine hydroxylase;
TNF-α

Tumor necrosis factor α;
CMC
Carboxymethyl cellulose;
PBMC
Peripheral blood mononuclear cell;
GAPDH
Glyceraldehyde-3-phosphate dehydrogenase;
WT-OX
Overexpressing human wild-type;
PCR
Polymerase chain reaction;
PBS
Phosphate-buffered saline;
CMC
Carboxymethyl cellulose;

Declarations

Ethical Approval and Consent to participate

All protocols were performed according to the Guide for the Care and Use of Laboratory Animals of Sun Yat-sen University (Guangzhou, China) Committee

Consent for publication

Not applicable.

Availability of data and materials

All data generated or analysed during this study are included in this published article [and its supplementary information files].

Competing interests

The authors declare that they have no competing interests.

Funding

This work was supported by the Grants from the National Key Research and Development Program of China Stem Cell and Translational Research (No. 2017YFA0105104) the National Natural Science Foundation of China (No. 8187375, No.81671102) Guangdong provincial science and technology plan project (No. 2016B030230002); the Southern China International Cooperation Base for Early Intervention and Functional Rehabilitation of Neurological Diseases (2015B050501003), Guangdong Provincial

Engineering Center For Major Neurological Disease Treatment, Guangdong Provincial Translational Medicine Innovation Platform for Diagnosis and Treatment of Major Neurological Disease, Guangdong Provincial Clinical Research Center for Neurological Diseases.

Authors' contributions

YKF, YWP and ZP figured and planned the experiments. YKF, QLW, FYL, HJY, YWF, GL, XJL , SHL , YCL and YZ implemented the experiments. YKF, QLW, HJY and YWF analyzed the data. YKF and ZP wrote the paper. All authors read and approved the final manuscript.

Corresponding author

Correspondence to Zhong Pei

Acknowledgements

We thank International Science Editing (http://www.internationalscienceediting.com) for editing this manuscript.

References

1. Kalia LV. A. E. Lang. Parkinson disease in 2015: Evolving basic, pathological and clinical concepts in PD. Nat Rev Neurol,2016,12(2): 65–66.
2. MacLeod D, Dowman J, Hammondet R. al. The familial Parkinsonism gene LRRK2 regulates neurite process morphology. Neuron,2006,52(4): 587–593.
3. Khan NL, Jain S, Lynchet JM al. Mutations in the gene LRRK2 encoding dardarin (PARK8) cause familial Parkinson's disease: clinical, pathological, olfactory and functional imaging and genetic data. Brain,2005,128(Pt 12): 2786–2796.
4. Gaig C, Ezquerra M, Martiet MJ. al. LRRK2 mutations in Spanish patients with Parkinson disease: frequency, clinical features, and incomplete penetrance. Arch Neurol,2006,63(3): 377–382.
5. Lee H, James WS, Cowley SA. LRRK2 in peripheral and central nervous system innate immunity: its link to Parkinson's disease. Biochem Soc Trans,2017,45(1): 131–139.
6. Kozina E, Sadasivan S, Jiaoet Y. al. Mutant LRRK2 mediates peripheral and central immune responses leading to neurodegeneration in vivo. Brain,2018,141(6): 1753–1769.
7. Fava VM, Manry J, Cobatet al A. A Missense LRRK2 Variant Is a Risk Factor for Excessive Inflammatory Responses in Leprosy. PLoS Negl Trop Dis. 2016;10(2):e4412.
8. Takagawa T, Kitani A, Fusset I. al. An increase in LRRK2 suppresses autophagy and enhances Dectin-1-induced immunity in a mouse model of colitis. Sci Transl Med,2018,10(444).
9. Liu W, Liu X, Liet Y. al. LRRK2 promotes the activation of NLRC4 inflammasome during Salmonella Typhimurium infection. J Exp Med,2017,214(10): 3051–3066.

10. Chou JS, Chen CY, Chenet al YL. (G2019S) LRRK2 causes early-phase dysfunction of SNpc dopaminergic neurons and impairment of corticostriatal long-term depression in the PD transgenic mouse. Neurobiol Dis. 2014;68:190–9.
11. Kaur T, Uppoor A, Naik D. Parkinson's disease and periodontitis - the missing link? A review. Gerodontology,2016,33(4): 434–438.
12. Hanaoka A, Kashihara K. Increased frequencies of caries, periodontal disease and tooth loss in patients with Parkinson's disease. J Clin Neurosci,2009,16(10): 1279–1282.
13. Einarsdottir ER, Gunnsteinsdottir H, Hallsdottiret MH. al. Dental health of patients with Parkinson's disease in Iceland. Spec Care Dentist,2009,29(3): 123–127.
14. Nakajima M, Arimatsu K, Katoet T. al. Oral Administration of P. gingivalis Induces Dysbiosis of Gut Microbiota and Impaired Barrier Function Leading to Dissemination of Enterobacteria to the Liver. PLoS One,2015,10(7): e134234.
15. Arimatsu K, Yamada H, Miyazawaet H. al. Oral pathobiont induces systemic inflammation and metabolic changes associated with alteration of gut microbiota. Sci Rep. 2014;4:4828.
16. Houser MC, Tansey MG. The gut-brain axis: is intestinal inflammation a silent driver of Parkinson's disease pathogenesis? NPJ Parkinsons Dis,2017,3: 3.
17. Timothy R, Sampson W. Debelius Taren Thron Justine, Zehra Esra Ilhan Collin Shastriet al. Gut Microbiota Regulate Motor Deficits and Neuroinflammation in a Model of Parkinson's Disease. Cell,2016,6(167): 1469–1480.
18. Suresh M, Czerwinski S, Murredduet MG. al. Innate and adaptive immunity associated with resolution of acute woodchuck hepatitis virus infection in adult woodchucks. PLoS Pathog. 2019;15(12):e1008248.
19. Sommer A, Maxreiter F, Krachet F. al. Th17 Lymphocytes Induce Neuronal Cell Death in a Human iPSC-Based Model of Parkinson's Disease. Cell Stem Cell,2018,23(1): 123–131.
20. Huang Y, Liu Z, Wanget XQ. al. A dysfunction of CD4 + T lymphocytes in peripheral immune system of Parkinson's disease model mice. Zhongguo Ying Yong Sheng Li Xue Za Zhi,2014,30(6): 567–576.
21. Green HF, Khosousi S, Svenningsson P. Plasma IL-6 and IL-17A Correlate with Severity of Motor and Non-Motor Symptoms in Parkinson's Disease. J Parkinsons Dis,2019,9(4): 705–709.
22. Linhartova P, Borilova J, Kastovsky S, Lucanovaet. al. Interleukin-17A Gene Variability in Patients with Type 1 Diabetes Mellitus and Chronic Periodontitis: Its Correlation with IL-17 Levels and the Occurrence of Periodontopathic Bacteria. Mediators Inflamm,2016,2016: 2979846.
23. Adibrad M, Deyhimi P, Hakemi M, Ganjalikhaniet. al. Signs of the presence of Th17 cells in chronic periodontal disease. J Periodontal Res,2012,47(4): 525–531.
24. Blaschitz C, Raffatellu M. Th17 cytokines and the gut mucosal barrier. J Clin Immunol,2010,30(2): 196–203.
25. Gerhard A, Pavese N. G. Hottonet al. In vivo imaging of microglial activation with [11C](R)-PK11195 PET in idiopathic Parkinson's disease. Neurobiol Dis. 2006;21(2):404–12.

26. Barcia C, Ros CM, Ros-Bernalet F. al. Persistent phagocytic characteristics of microglia in the substantia nigra of long-term Parkinsonian macaques. J Neuroimmunol. 2013;261(1–2):60–6.
27. Ma Y, Zheng C, Shi L. The kinase LRRK2 is differently expressed in chronic rhinosinusitis with and without nasal polyps. Clinical and Translational Allergy,2018,8(1).
28. Yuki Kishimoto W, Zhu. Waki Hosodaet al. Chronic Mild Gut Inflammation Accelerates Brain Neuropathology and Motor Dysfunction in α – Synuclein Mutant Mice. NeuroMolecular Medicine,2019.
29. Hakimi M, Selvanantham T, Swintonet E. al. Parkinson's disease-linked LRRK2 is expressed in circulating and tissue immune cells and upregulated following recognition of microbial structures. J Neural Transm (Vienna),2011,118(5): 795–808.
30. Liu Z, Lee J, Krummeyet S. al. The kinase LRRK2 is a regulator of the transcription factor NFAT that modulates the severity of inflammatory bowel disease. Nat Immunol. 2011;12(11):1063–70.
31. Kelly LP, Carvey PM, Keshavarzianet A. al. Progression of intestinal permeability changes and alpha-synuclein expression in a mouse model of Parkinson's disease. Mov Disord,2014,29(8): 999–1009.
32. Houser MC, Tansey MG. The gut-brain axis: is intestinal inflammation a silent driver of Parkinson's disease pathogenesis? NPJ Parkinsons Dis,2017,3: 3.
33. Volpicelli-Daley LA, Abdelmotilib H, Liuet al Z. G2019S-LRRK2 Expression Augments alpha-Synuclein Sequestration into Inclusions in Neurons. J Neurosci,2016,36(28): 7415–7427.
34. J. P. Daher. Interaction of LRRK2 and alpha-Synuclein in Parkinson's Disease. Adv Neurobiol,2017,14: 209–226.
35. Kim S, Kwon SH, Kamet TI. al. Transneuronal Propagation of Pathologic alpha-Synuclein from the Gut to the Brain Models Parkinson's Disease. Neuron,2019,103(4): 627–641.
36. Maes M, Kubera M, Leunis JC. The gut-brain barrier in major depression: intestinal mucosal dysfunction with an increased translocation of LPS from gram negative enterobacteria (leaky gut) plays a role in the inflammatory pathophysiology of depression. Neuro Endocrinol Lett,2008,29(1): 117–124.
37. Gibson PR. Increased gut permeability in Crohn's disease: is TNF the link? Gut,200453(12): 1724–1725.
38. Hakimi M, Selvanantham T, Swintonet E. al. Parkinson's disease-linked LRRK2 is expressed in circulating and tissue immune cells and upregulated following recognition of microbial structures. J Neural Transm (Vienna),2011,118(5): 795–808.
39. Sun J, Zhang S, Zhanget al X. IL-17A is implicated in lipopolysaccharide-induced neuroinflammation and cognitive impairment in aged rats via microglial activation. J Neuroinflammation. 2015;12:165.
40. Waisman A, Hauptmann J, Regen T. The role of IL-17 in CNS diseases. Acta Neuropathol,2015,129(5): 625–637.
41. Liu Z, Qiu AW, Huanget Y. al. IL-17A exacerbates neuroinflammation and neurodegeneration by activating microglia in rodent models of Parkinson's disease. Brain Behav Immun,2019,81: 630–645.

42. Kebir H, Kreymborg K, Iferganet I. al. Human TH17 lymphocytes promote blood-brain barrier disruption and central nervous system inflammation. Nat Med,2007,13(10): 1173–1175.
43. Jill F, Wright F, Bennett B. Liet al. The Human IL-17F/IL-17A Heterodimeric Cytokine Signals through the IL-17RA/IL-17RC Receptor Complex. The Journal of Immunology,2008,181(4.): 2799–2805.
44. Dilger RN. R. W. Johnson. Aging, microglial cell priming, and the discordant central inflammatory response to signals from the peripheral immune system. J Leukoc Biol,2008,84(4): 932–939.
45. Li T, Yang D, Zhonget S. al. Novel LRRK2 GTP-binding inhibitors reduced degeneration in Parkinson's disease cell and mouse models. Hum Mol Genet,2014,23(23): 6212–6222.
46. Gillardon F, Schmid R, Draheim H. Parkinson's disease-linked leucine-rich repeat kinase 2(R1441G) mutation increases proinflammatory cytokine release from activated primary microglial cells and resultant neurotoxicity. Neuroscience,2012,208: 41–48.

Figures

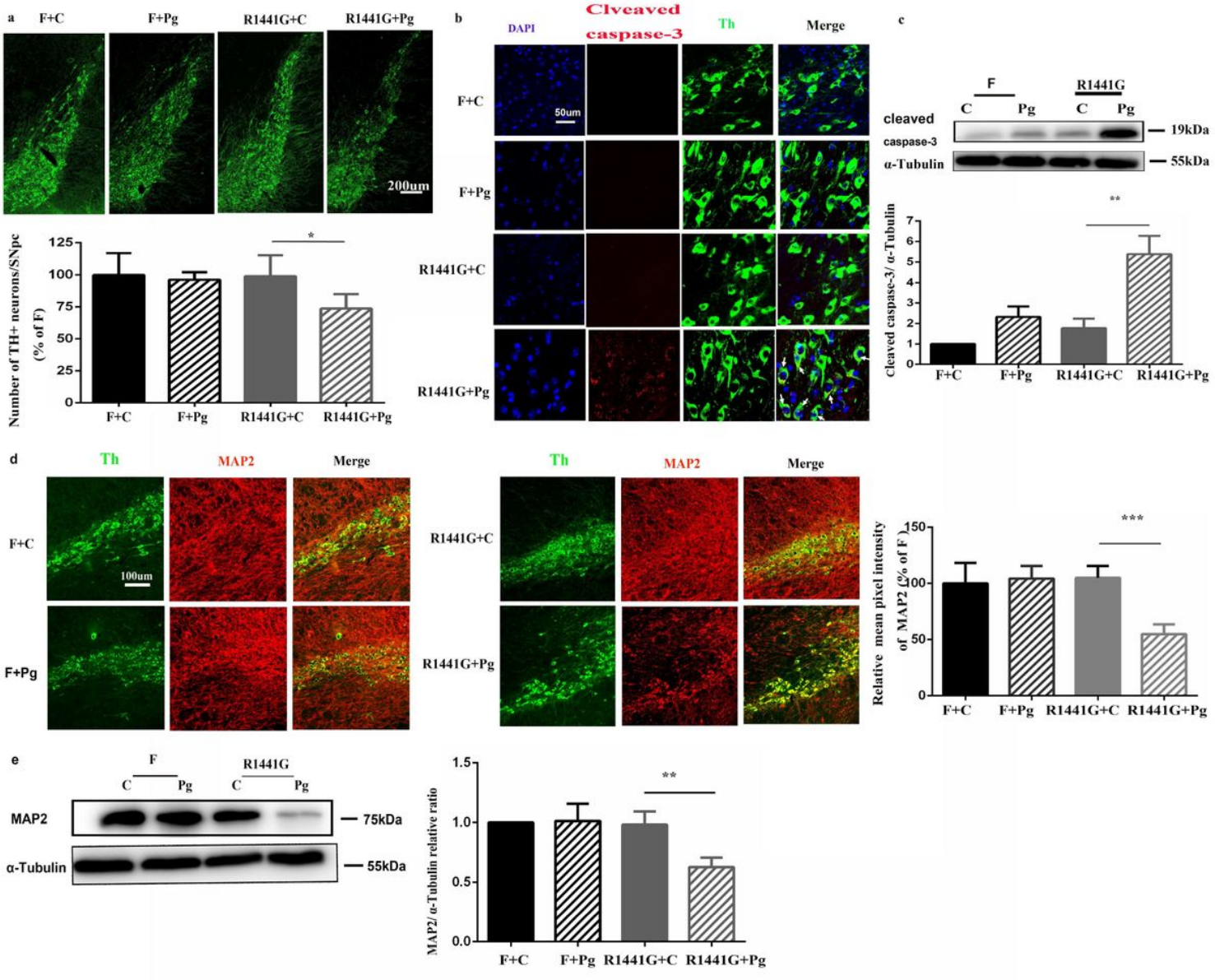

Figure 1

Oral Pg induced dopaminergic neuronal degeneration in the SNpc of mutant LRRK2 mice. (a) Representative images of immunofluorescence-stained coronal brain sections and quantification of TH number (a marker of dopaminergic neuron) from F + Pg and R1441G + Pg groups compared to F + C and R1441G + C mice. n = 4–5, * P < 0.05. (Scale bar = 200 μm.) (b) Representative images of TH+ dopaminergic neurons (green) and cleaved caspase-3 (red) (white arrows indicate colocalized cells) immunofluorescent staining from the SN in brain sections obtained from F + C, F + Pg, R1441G + Pg, and R1441G + C mice. (Scale bar = 50 μm.) (c) Representative images of western blots of cleaved caspase-3 protein levels and quantitative analysis, which were done with the SN obtained from F + Pg and 1441 + Pg mice compared to F + C and 1441 + C mice, n = 4, **P < 0.01. (d) Representative images of immunofluorescence double staining with dendric marker MAP2 and comparison of dendric density from F + Pg, 1441 + Pg, F + C, and 1441 + C mice. n = 4–5, ***P < 0.001. (Scale bar = 100 μm.) (e) Representative images of western blots and quantitative analyses of MAP2 protein levels. Analyses of protein levels of MAP2 were done on the SN obtained from F + Pg and 1441 + Pg mice compared to F + C and 1441 + C mice, n = 4, **P < 0.01.

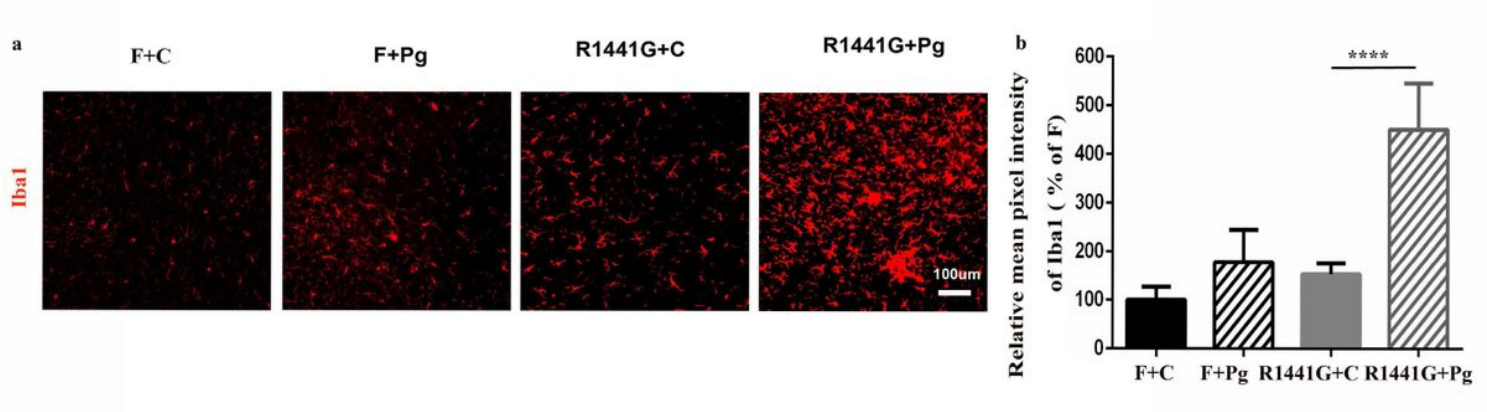

Figure 2

Oral Pg increased microglial activation in the SNpc of mutant LRRK2 mice (a) Representative images of immunofluorescence staining with Iba1 (a marker of microglia) and comparison of Iba1 density (b) in the SN area from F + Pg and 1441 + Pg mice compared to F + C and 1441 + C mice. n = 4–5, ****P < 0. 0001. (Scale bar = 100 μm.)

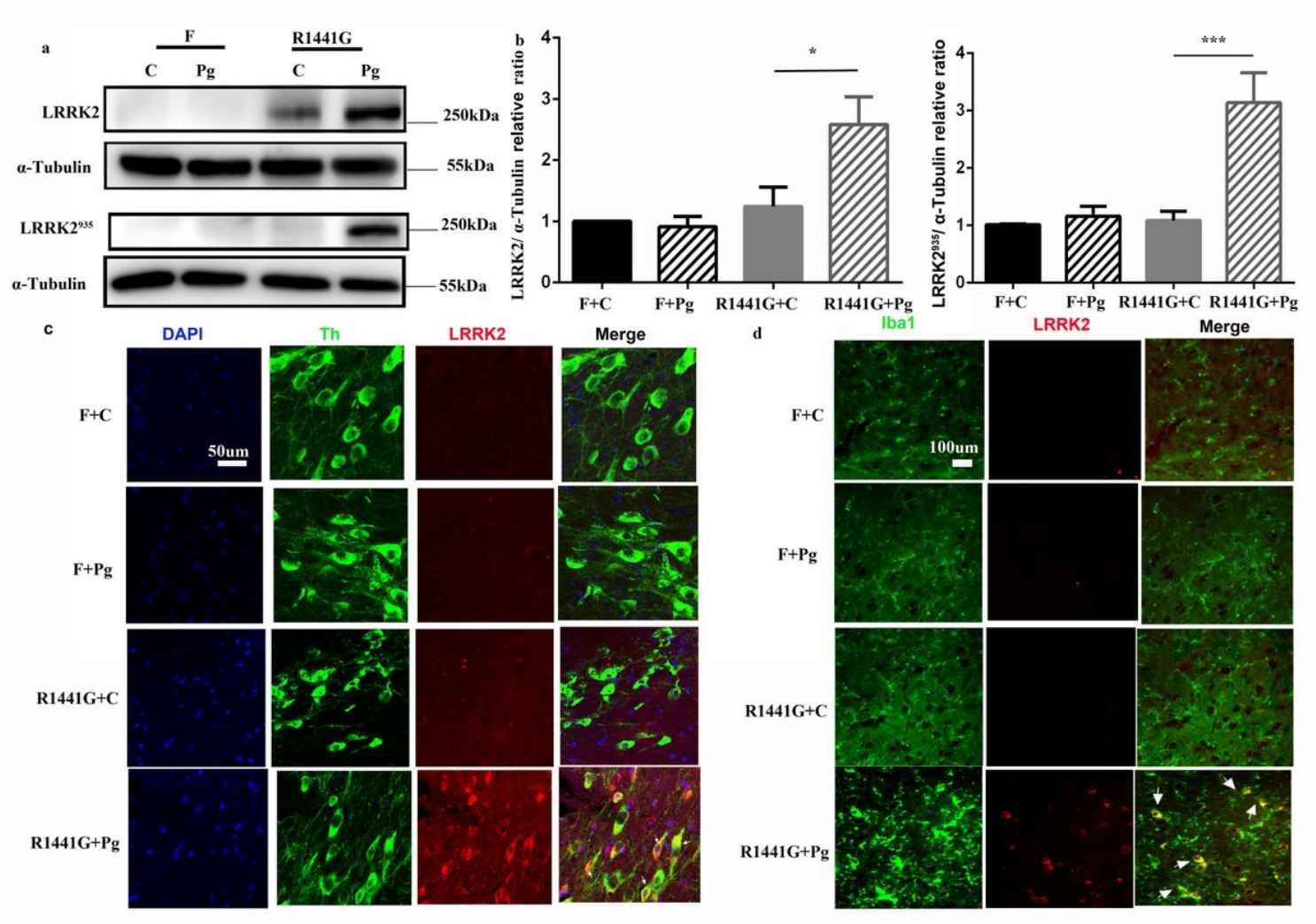

Figure 3

Oral Pg increased LRRK2 activation in the SN of R1441G mice (a) Representative images of western blots of LRRK2 and LRRK935 protein levels and (b) quantitative analysis, which were done on the SN obtained from F + Pg and 1441 + Pg mice compared to F + C and 1441 + C mice, n = 4, ***P < 0.001,* P < 0.05. (c) Representative images of TH+ dopaminergic neuron by immunofluorescent double staining with LRRK2 (white arrows indicate colocalized cells). (Scale bar = 50 μm.) (d) Representative images of Iba1+ microglia by immunofluorescent double staining with LRRK2 (white arrows indicate the cells co-localized with LRRK2 and Iba1). (Scale bar = 100 μm.)

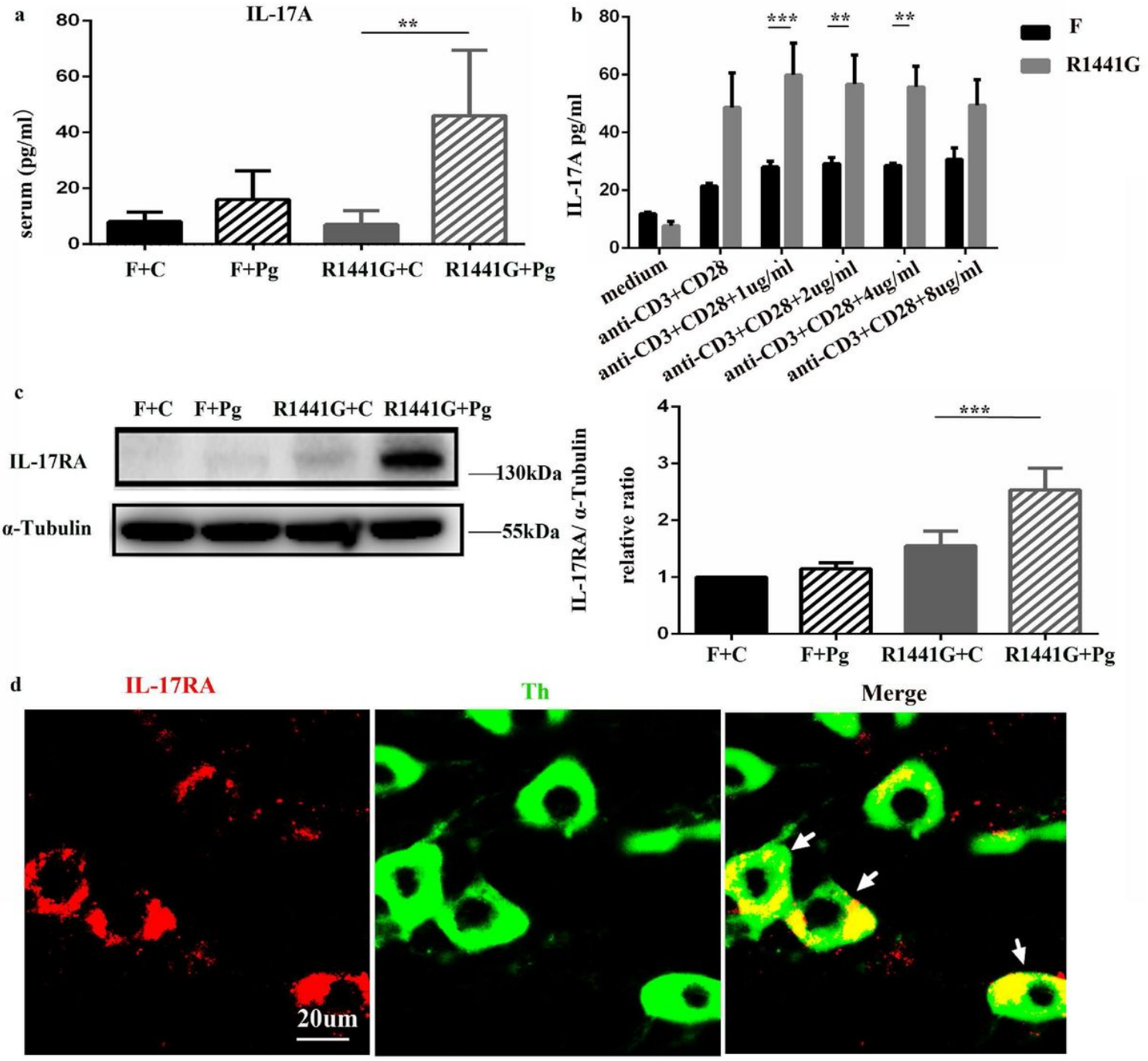

Figure 4

Mutant LRRK2 exacerbated Pg-induced peripheral IL-17A secretion and IL-17RA upregulation The mice were equally divided into four groups, F + C, F + Pg, 1441 + C, and 1441 + Pg. IL-17A protein levels in serum (a) were examined using ELISA. n = 4–5, **P < 0.01. (b) Pg-treated PBMC were stimulated for about 24 h and the IL-17A protein levels in the supernatant were measured by ELISA. n = 3, **P < 0.01, ***P < 0.001. (c) Representative images of western blot of IL-17RA obtained from SN tissue and quantitative analysis, n = 4, ***P < 0.001. (d) Representative images of co-localization of TH (green) and IL-17RA (red) from Pg-treated R1441G mice.

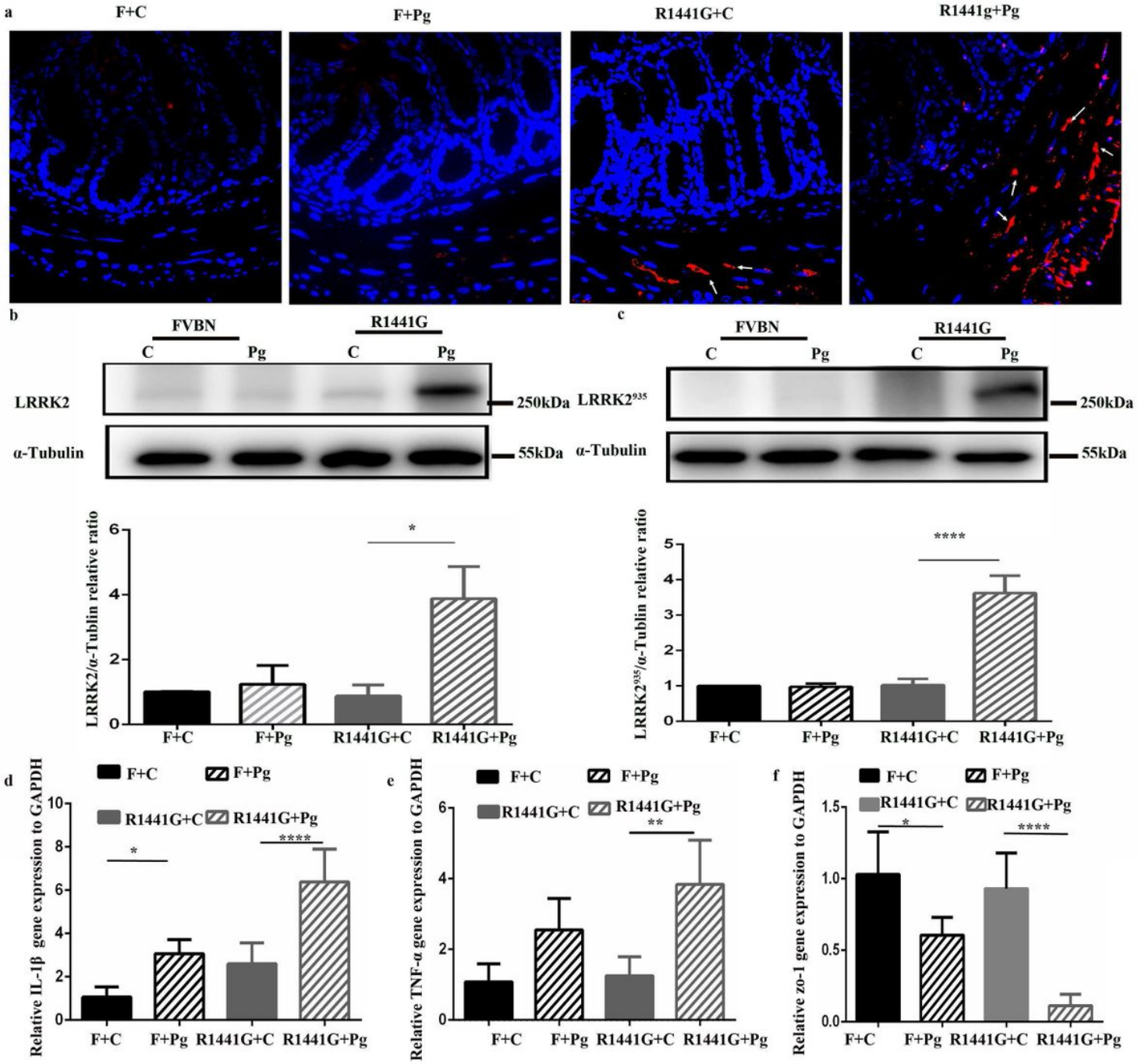

Figure 5

Pg-treatment increased the accumulation of α-synuclein in neurons of the colon and caused activation of LRRK2 (a) Representative images of α-synuclein (red) (white arrows) immunofluorescent staining from the colon obtained from F + C, F + Pg, 1441 + Pg, and 1441 + C mice. (Scale bar = 100 μm.) Representative images of western blots of (b) LRRK2 and (c) LRRK935 protein levels, and quantitative analysis, which were done with the colon tissue obtained from F + Pg and 1441 + Pg groups and compared with F + C and 1441 + C mice, n = 4, ****P < 0.0001,* P < 0.05. Comparison of relative (d) IL-1β, (e) TNF-α, and (f) Zo-1 gene expression levels in the colon from F + C, F + Pg, 1441 + Pg, and 1441 + C mice, n = 6–8, * P < 0.05, **P < 0.01, ****P < 0.0001.

Supplementary Files

This is a list of supplementary files associated with this preprint. Click to download.

- supplement9.pdf
- supplement10.pdf
- supplement11.pdf
- supplement12.doc